Free Energies and Phase Transitions in Materials with Hysteresis

Claudio Giorgi*

Alessia Berti† and Elena Vuk*

* Dipartimento di Matematica, Università di Brescia

† Facoltà di Ingegneria, Università e-Campus

PDEs for Advanced Materials

ADMAT 2012

Cortona, September 17-21 2012

- A lot of physical an biological phenomena exhibits hysteresis (elasto-plasticity, ferromagnetism, biochemical oscillators,...)
- Many mathematical models for hysteresis have been proposed in the literature, most of which are devoted to ferromagnetic bodies (Coleman-Hodgdon, Jiles-Atherton, Preisach,...)
- But few of them describes the temperature-induced phase transition between the non-hysteretic (paramagnetic) and the hysteretic (ferromagnetic) regimes.

Introduction

- A lot of physical an biological phenomena exhibits hysteresis (elasto-plasticity, ferromagnetism, biochemical oscillators,...)
- Many mathematical models for hysteresis have been proposed in the literature, most of which are devoted to ferromagnetic bodies (Coleman-Hodgdon, Jiles-Atherton, Preisach,...)
- But few of them describes the temperature-induced phase transition between the non-hysteretic (paramagnetic) and the hysteretic (ferromagnetic) regimes.

Introduction

- A lot of physical an biological phenomena exhibits hysteresis (elasto-plasticity, ferromagnetism, biochemical oscillators,...)
- Many mathematical models for hysteresis have been proposed in the literature, most of which are devoted to ferromagnetic bodies (Coleman-Hodgdon, Jiles-Atherton, Preisach,...)
- But few of them describes the temperature-induced phase transition between the non-hysteretic (paramagnetic) and the hysteretic (ferromagnetic) regimes.

Introduction

Recently, some efforts have been made in order to apply the Ginzburg-Landau theory to model temperature-induced phase transitions with hysteresis:

1. Fabrizio, – , Morro, Phase transition in ferromagnetism, *Internat. J. Engrg. Sci.*, 47 (2009) 821–839.
2. Berti A., – , Vuk, Free energies and pseudo-elastic transitions for Shape Memory Alloys, *DCDS–S in honor to M.Frémond*, to appear.
3. Berti A., – , Vuk, Hysteresis and thermally-induced transitions in ferromagnetic materials, in preparation

Recently, some efforts have been made in order to apply the Ginzburg-Landau theory to model temperature-induced phase transitions with hysteresis:

1. Fabrizio, – , Morro, Phase transition in ferromagnetism, *Internat. J. Engrg. Sci.*, 47 (2009) 821–839.
2. Berti A., – , Vuk, Free energies and pseudo-elastic transitions for Shape Memory Alloys, *DCDS–S in honor to M.Frémond*, to appear.
3. Berti A., – , Vuk, Hysteresis and thermally-induced transitions in ferromagnetic materials, in preparation

Recently, some efforts have been made in order to apply the Ginzburg-Landau theory to model temperature-induced phase transitions with hysteresis:

1. Fabrizio, – , Morro, Phase transition in ferromagnetism, *Internat. J. Engrg. Sci.*, 47 (2009) 821–839.
2. Berti A., – , Vuk, Free energies and pseudo-elastic transitions for Shape Memory Alloys, *DCDS–S in honor to M.Frémond*, to appear.
3. Berti A., – , Vuk, Hysteresis and thermally-induced transitions in ferromagnetic materials, in preparation

Recently, some efforts have been made in order to apply the Ginzburg-Landau theory to model temperature-induced phase transitions with hysteresis:

1. Fabrizio, – , Morro, Phase transition in ferromagnetism, *Internat. J. Engrg. Sci.*, 47 (2009) 821–839.
2. Berti A., – , Vuk, Free energies and pseudo-elastic transitions for Shape Memory Alloys, *DCDS–S in honor to M.Frémond*, to appear.
3. Berti A., – , Vuk, Hysteresis and thermally-induced transitions in ferro-magnetic materials, in preparation

- **Transitions without hysteresis.**
  Pressure-induced liquid/vapor transition (first order)

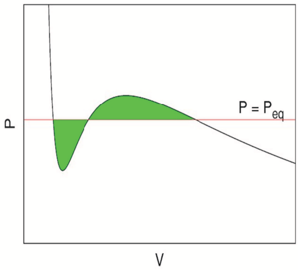

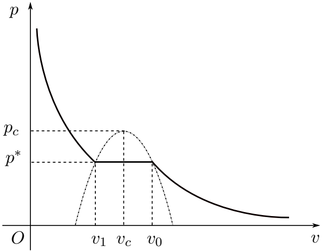

Figure: Maxwell construction of the Amagat-Andrews diagram

- **Transitions without hysteresis.**
  Thermodynamic potential ψ (double-well shaped)
  $\varphi = -1$ vapor, $\varphi = 1$ liquid

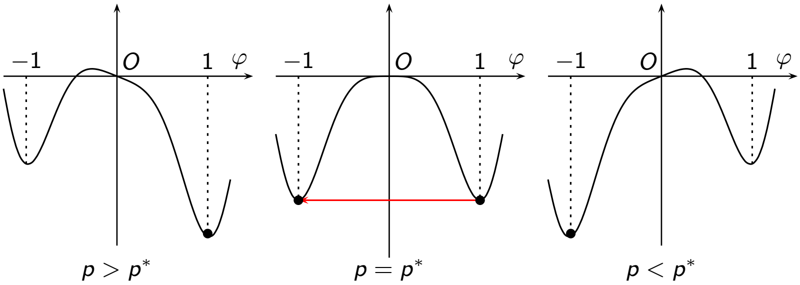

- **Transitions with hysteresis**:
  1 – Stress-induced austenite/martensite transition
  Shape memory alloys (pseudo-elastic regime: $\theta > \theta_c$)

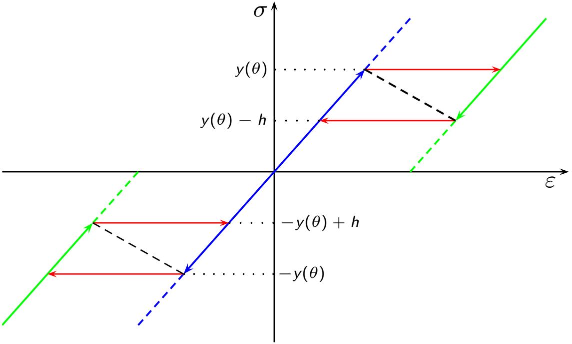

Figure: Stable (solid) and unstable (dashed) equilibrium branches.

- **Transitions with hysteresis**:
  1 – Stress-induced austenite/martensite transition
  Shape memory alloys (pseudo-elastic regime: $\theta > \theta_c$)

more regular ...

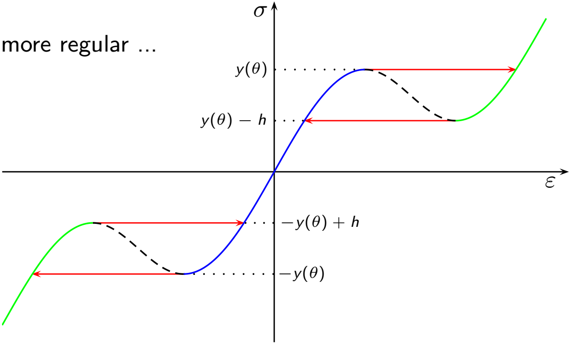

Figure: Stable (solid) and unstable (dashed) equilibrium branches.

- **Transitions with hysteresis**:
  1 – Stress-induced austenite/martensite transition
  Thermodynamic potential ψ (double-well shaped)
  $\varphi = 0$ austenite, $\varphi = \pm 1$ martensite

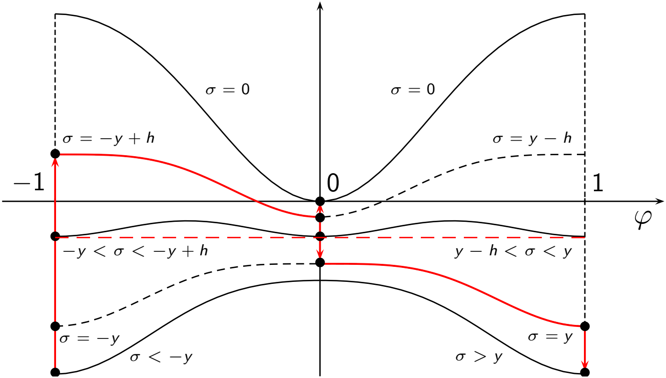

Isothermal transitions

- **Transitions with hysteresis**:
  2 – H-induced transition ($H =$ external field)
  Ferromagnetic materials (ferromagnetic regime: $\theta < \theta_c$)

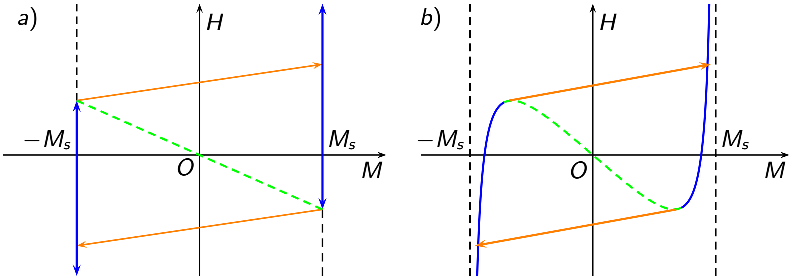

Figure: The major hysteresis loop: a) bilinear and b) Langevin.

- **Transitions with hysteresis**:
  2 – H-induced transition ($\tilde{H} =$ internal field)
  Ferromagnetic materials (ferromagnetic regime: $\theta < \theta_c$)

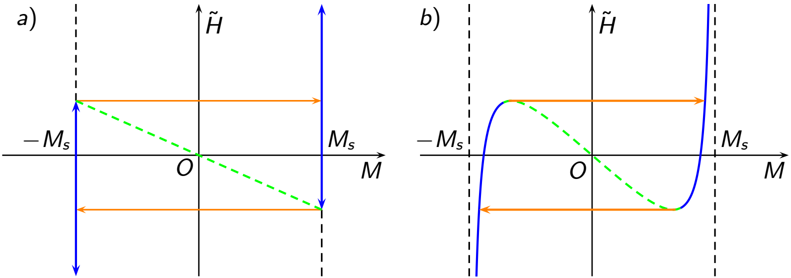

Figure: The major hysteresis loop: a) bilinear and b) Langevin.

Plan

1. Duhem's rate-independent models are considered

$$\frac{dM}{dH} = \mathcal{F}(M, H, \operatorname{sgn} \dot{H}), \qquad \operatorname{sgn} P = \begin{cases} +1 & \text{if } P > 0, \\ 0 & \text{if } P = 0, \\ -1 & \text{if } P < 0. \end{cases}$$

   M - magnetization, H - applied magnetic field,
   $\chi = dM/dH$ - magnetic susceptibility

2. The role of skeleton curve description is emphasized.
3. The minimum (Gibbs) free energy representation is obtained: it is proved to be uniquely determined by the skeleton curve.
4. The Ginzburg-Landau framework for phase transitions in materials with hysteresis is derived.

1 – Bilinear model

$$\frac{dM}{dH} = \begin{cases} \chi & \text{if} \quad M = f_b(H)\,,\ |M| < M_s,\ \text{or} \\ & \quad\ M = f_b(H)\,,\ |M| = M_s \text{ and } M\,\mathrm{sgn}\,\dot{H} < 0,\ \text{or} \\ & \quad\ M \neq f_b(H) \text{ and } [f_b(H) - M]\,\mathrm{sgn}\,\dot{H} > 0, \\ 0 & \text{otherwise.} \end{cases}$$

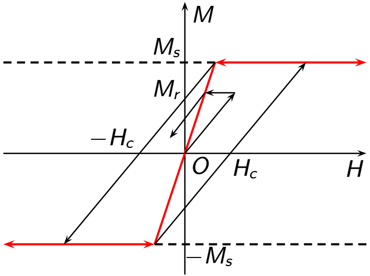

Figure: Major loop and hysteresis path (arrowhead) in the bilinear model (skeleton curve $f = f_b$ is red).

2 – Coleman & Hodgdon model (with a bilinear skeleton f_b)

$$\frac{dM}{dH} = \alpha[f(H) - M]\operatorname{sgn}\dot{H} + g(H).$$

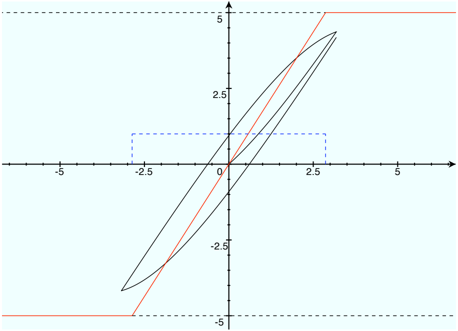

Figure: The Coleman-Hodgdon model (skeleton curve $f = f_b$ in red and fatness $g = g_b$ in blue.

3 – Coleman & Hodgdon model (with a Langevin skeleton f_L)

$$\frac{dM}{dH} = \alpha[f(H) - M]\mathrm{sgn}\,\dot{H} + g(H).$$

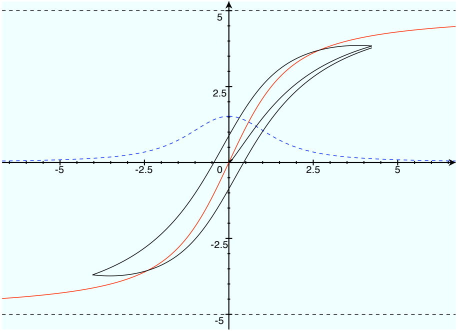

Figure: The Coleman-Hodgdon model (skeleton curve $f = f_L$ in red and fatness $g = g_L$ in blue.

The role of the skeleton curve

- The slope of the skeleton curve at $H = 0$ depends on the temperature:

$$\chi|_{H=0} = \chi_s(\theta) = \frac{\chi_0(\theta)}{1 + \gamma\chi_0(\theta)}\,, \quad \chi_0(\theta) = \frac{C}{\theta}\,,\ \gamma = \alpha - \frac{\theta_c}{C}\,,$$

- In the limit of high temperatures $\chi_s(\theta) \approx C/(\theta - \theta_c)$ (Curie-Weiss law)
- There is a critical temperature, θ_c, and a critical slope, $\boxed{\chi_s(\theta_c) = 1/\alpha}$, at which transition to hysteresis occurs.
- Soft materials: $\lim_{\theta\to 0} \chi_s(\theta) = 1/\gamma > 0$,
- Hard materials: $\lim_{\theta\to 0} \chi_s(\theta) = 1/\gamma < 0$,

The role of the skeleton curve

- The slope of the skeleton curve at $H = 0$ depends on the temperature:

$$\chi|_{H=0} = \chi_s(\theta) = \frac{\chi_0(\theta)}{1 + \gamma\chi_0(\theta)}, \quad \chi_0(\theta) = \frac{C}{\theta}, \ \gamma = \alpha - \frac{\theta_c}{C},$$

- In the limit of high temperatures $\chi_s(\theta) \approx C/(\theta - \theta_c)$ (Curie-Weiss law)
- There is a critical temperature, θ_c, and a critical slope, $\boxed{\chi_s(\theta_c) = 1/\alpha}$, at which transition to hysteresis occurs.
- Soft materials: $\lim_{\theta \to 0} \chi_s(\theta) = 1/\gamma > 0$,
- Hard materials: $\lim_{\theta \to 0} \chi_s(\theta) = 1/\gamma < 0$,

The role of the skeleton curve

- The slope of the skeleton curve at $H = 0$ depends on the temperature:

$$\chi|_{H=0} = \chi_s(\theta) = \frac{\chi_0(\theta)}{1 + \gamma\chi_0(\theta)}, \quad \chi_0(\theta) = \frac{C}{\theta}, \; \gamma = \alpha - \frac{\theta_c}{C},$$

- In the limit of high temperatures $\chi_s(\theta) \approx C/(\theta - \theta_c)$ (Curie-Weiss law)
- There is a critical temperature, θ_c, and a critical slope, $\boxed{\chi_s(\theta_c) = 1/\alpha}$, at which transition to hysteresis occurs.
- Soft materials: $\lim_{\theta\to 0} \chi_s(\theta) = 1/\gamma > 0$,
- Hard materials: $\lim_{\theta\to 0} \chi_s(\theta) = 1/\gamma < 0$,

The role of the skeleton curve

- The slope of the skeleton curve at $H = 0$ depends on the temperature:

$$\chi|_{H=0} = \chi_s(\theta) = \frac{\chi_0(\theta)}{1+\gamma\chi_0(\theta)}, \quad \chi_0(\theta) = \frac{C}{\theta}, \ \gamma = \alpha - \frac{\theta_c}{C},$$

- In the limit of high temperatures $\chi_s(\theta) \approx C/(\theta - \theta_c)$ (Curie-Weiss law)
- There is a critical temperature, θ_c, and a critical slope, $\boxed{\chi_s(\theta_c) = 1/\alpha}$, at which transition to hysteresis occurs.
- Soft materials: $\lim_{\theta\to 0} \chi_s(\theta) = 1/\gamma > 0$,
- Hard materials: $\lim_{\theta\to 0} \chi_s(\theta) = 1/\gamma < 0$,

2.1 - The role of the skeleton curve: the bilinear case

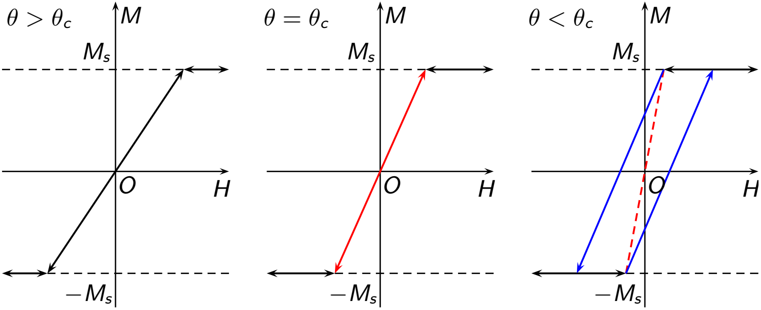

Figure: The bilinear-model transition: the critical slope (in red).

2.2 - The role of the skeleton curve: the Langevin case

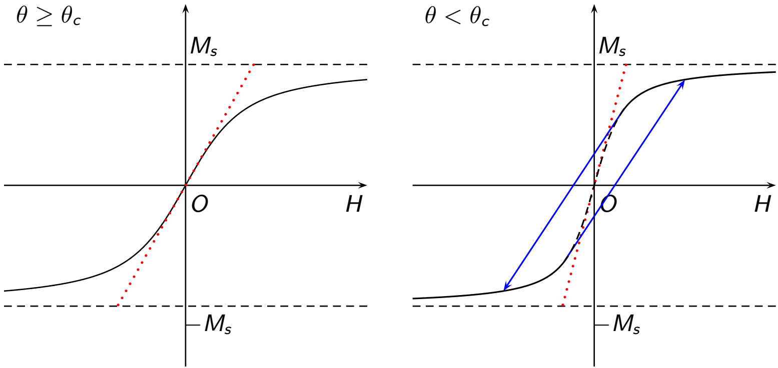

Figure: The Langevin-model transition: the slope $\chi|_{H=0}$ (dotted red).

2.3 - The role of the skeleton curve: soft and hard ferromagnetics

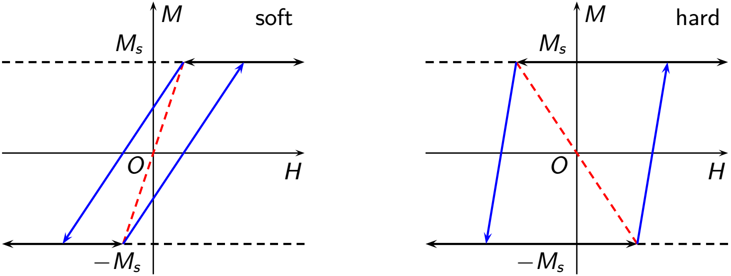

$\chi_s \approx \frac{1}{\gamma} > 0$ $\qquad$ $\chi_s \approx \frac{1}{\gamma} < 0$

Figure: The bilinear-model transition: the skeleton slope when $\theta \approx 0$ (in red).

- *Internal magnetic field* $\tilde{\mathbf{H}}$ (Brown, 1963):

$$\tilde{\mathbf{H}} = \mathbf{H} - \mathbb{A}\mathbf{M},$$

$\mathbb{A}$ is a positive-definite tensor which depends on the shape and the anisotropy of the material.

- Along a fixed direction (eigenvector)

$$\boxed{\tilde{H} = H - \alpha M}, \qquad \alpha > 0$$

- Paramagnetic relation (Coey, 2009)

$$M = f(\tilde{H}, \theta) = f(H - \alpha M, \theta), \qquad f(0, \cdot) = 0\,.$$

and

$$\chi(H, \theta) = \partial_{\tilde{H}} f(\tilde{H}, \theta)$$

- *Internal magnetic field* $\tilde{\mathbf{H}}$ (Brown, 1963):

$$\tilde{\mathbf{H}} = \mathbf{H} - \mathbb{A}\mathbf{M},$$

  $\mathbb{A}$ is a positive-definite tensor which depends on the shape and the anisotropy of the material.

- Along a fixed direction (eigenvector)

$$\boxed{\tilde{H} = H - \alpha M}, \qquad \alpha > 0$$

- *Paramagnetic relation* (Coey, 2009)

$$M = f(\tilde{H}, \theta) = f(H - \alpha M, \theta), \qquad f(0, \cdot) = 0\,.$$

and

$$\chi(H, \theta) = \partial_{\tilde{H}} f(\tilde{H}, \theta)$$

- *Internal magnetic field* $\tilde{\mathbf{H}}$ (Brown, 1963):

$$\tilde{\mathbf{H}} = \mathbf{H} - \mathbb{A}\mathbf{M},$$

  $\mathbb{A}$ is a positive-definite tensor which depends on the shape and the anisotropy of the material.

- Along a fixed direction (eigenvector)

$$\boxed{\tilde{H} = H - \alpha M}, \qquad \alpha > 0$$

- Paramagnetic relation (Coey, 2009)

$$M = f(\tilde{H}, \theta) = f(H - \alpha M, \theta), \qquad f(0, \cdot) = 0\,.$$

  and

$$\chi(H, \theta) = \partial_{\tilde{H}} f(\tilde{H}, \theta)$$

By reversing the paramagnetic relation we have

$$H = f^{-1}(M,\theta) + \alpha M$$

and then

$$M = \tilde{f}(H,\theta)\,, \qquad \tilde{\chi}(H,\theta) = \partial_H \tilde{f}(H,\theta)$$

$$\boxed{\tilde{\chi}|_{H=0} = \frac{\chi_s(\theta)}{1-\alpha\chi_s(\theta)}}\,, \quad \alpha = \frac{1}{\chi_s(\theta_c)}\,,$$

- The critical slope $\tilde{\chi}|_{H=0}$ at $\theta = \theta_c$ becomes a vertical line.
- In the limit of high temperatures $\tilde{\chi}(0,\theta) \approx C/(\theta-\theta_c)$ (Curie-Weiss law)

By reversing the paramagnetic relation we have

$$H = f^{-1}(M, \theta) + \alpha M$$

and then

$$M = \tilde{f}(H, \theta), \qquad \tilde{\chi}(H, \theta) = \partial_H \tilde{f}(H, \theta)$$

$$\boxed{\tilde{\chi}|_{H=0} = \frac{\chi_s(\theta)}{1 - \alpha \chi_s(\theta)}}, \quad \alpha = \frac{1}{\chi_s(\theta_c)},$$

- The critical slope $\tilde{\chi}|_{H=0}$ at $\theta = \theta_c$ becomes a vertical line.
- In the limit of high temperatures $\tilde{\chi}(0, \theta) \approx C/(\theta - \theta_c)$ (Curie-Weiss law)

By reversing the paramagnetic relation we have

$$H = f^{-1}(M, \theta) + \alpha M$$

and then

$$M = \tilde{f}(H, \theta)\,, \qquad \tilde{\chi}(H, \theta) = \partial_H \tilde{f}(H, \theta)$$

$$\boxed{\tilde{\chi}|_{H=0} = \frac{\chi_s(\theta)}{1 - \alpha\chi_s(\theta)}}\,, \quad \alpha = \frac{1}{\chi_s(\theta_c)}\,,$$

- The critical slope $\tilde{\chi}|_{H=0}$ at $\theta = \theta_c$ becomes a vertical line.
- In the limit of high temperatures $\tilde{\chi}(0, \theta) \approx C/(\theta - \theta_c)$ (Curie-Weiss law)

By reversing the paramagnetic relation we have

$$H = f^{-1}(M, \theta) + \alpha M$$

and then

$$M = \tilde{f}(H, \theta)\,, \qquad \tilde{\chi}(H, \theta) = \partial_H \tilde{f}(H, \theta)$$

$$\boxed{\tilde{\chi}|_{H=0} = \frac{\chi_s(\theta)}{1 - \alpha\chi_s(\theta)}}\,, \quad \alpha = \frac{1}{\chi_s(\theta_c)}\,,$$

- The critical slope $\tilde{\chi}|_{H=0}$ at $\theta = \theta_c$ becomes a vertical line.
- In the limit of high temperatures $\tilde{\chi}(0, \theta) \approx C/(\theta - \theta_c)$ (Curie-Weiss law)

Temperature-induced transitions in the $\tilde{H} - M$ plane

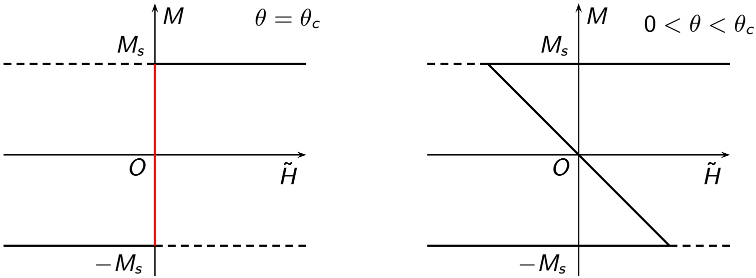

Figure: The graph of the bilinear skeleton curve referred to the internal field.

Temperature-induced transitions in the $\tilde{H} - M$ plane

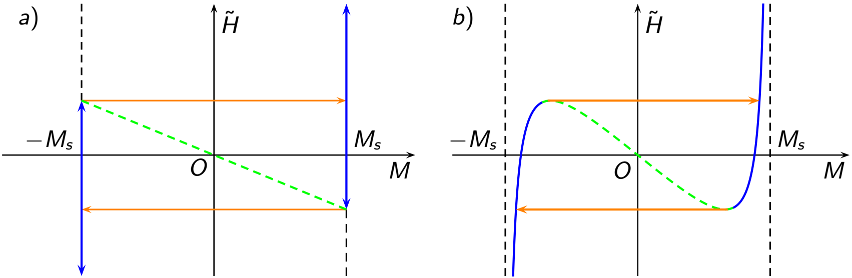

Figure: The major hysteresis loop when $0 < \theta < \theta_c$: a) bilinear and b) Langevin.

Letting

$$m = \frac{M}{M_s}, \qquad |m| \leq 1,$$

from the general theory (Fabrizio,–, Morro, 2009)

$$\dot{m} = -\omega\theta\,\delta_m \hat{\psi}_G = -\omega[\partial_m \hat{\psi}_G - \nabla \cdot \partial_{\nabla m} \hat{\psi}_G,]\,,$$

$\hat{\psi}_G = \dfrac{\psi_G}{\theta}$ – rescaled Gibbs free energy ,

$$\psi_G = \psi - \tilde{H}B = V(M,\theta) + \frac{1}{2}\kappa(\theta)|\nabla M|^2 - \frac{1}{2}\mu_0 \tilde{H}^2 - \mu_0 \tilde{H} M\,,$$

$$\dot{m} = -\hat{\omega}\left[\partial_M V - \mu_0 \tilde{H} - \theta \nabla \cdot (\hat{\kappa} \nabla M)\right]\,, \qquad \hat{\kappa} = \frac{\kappa}{\theta}\,, \quad \hat{\omega} = \omega\, M_s\,.$$

Assuming uniform fields ($\nabla M = \mathbf{0}$)

$$\dot{m} = -\hat{\omega}\left[\partial_M V - \mu_0 \tilde{H}\right] = -\hat{\omega}\,\partial_M \Phi,$$

where

$$\Phi(\tilde{H}, M, \theta) = V(M, \theta) - \mu_0 \tilde{H} M$$

can be identified with the Lagrangian density.

- Problem: the expression of V and Φ
- V can be uniquely determined from the skeleton curve: $dV = \mu_0 \tilde{H} dM = \mu_0 f^{-1}(M, \theta) dM$
- Φ can be uniquely identified (to within a function of $\tilde{H}$) as the minimum Gibbs free energy
  Remark: $\Phi(0, M, \theta) = V(M, \theta)$

Convex potentials V: $\theta > \theta_c$, $\boxed{\tilde{H} = 0}$

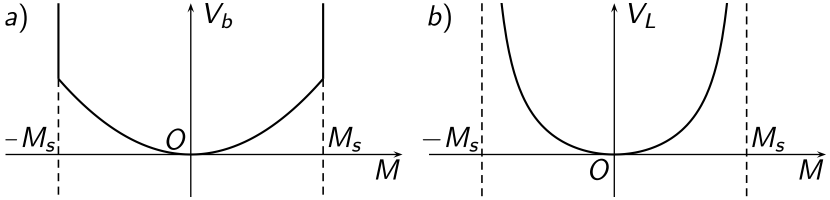

Figure: The graph of $V_b(\cdot, \theta)$ and $V_L(\cdot, \theta)$ when $\theta > \theta_c$.

Non-convex potentials V: $\theta < \theta_c$, $\boxed{\tilde{H} = 0}$

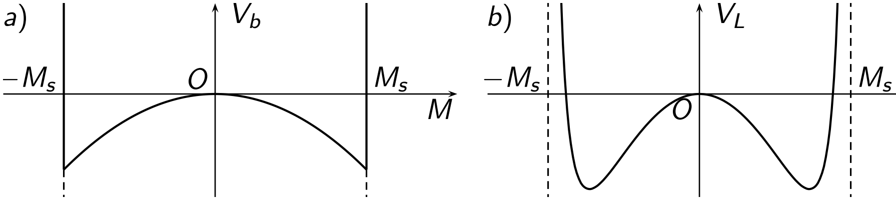

Figure: The graph of $V_b(\cdot, \theta)$ and $V_L(\cdot, \theta)$ when $0 < \theta < \theta_c$.

Convex potentials Φ: $\theta > \theta_c$, $\boxed{\tilde{H} > 0}$

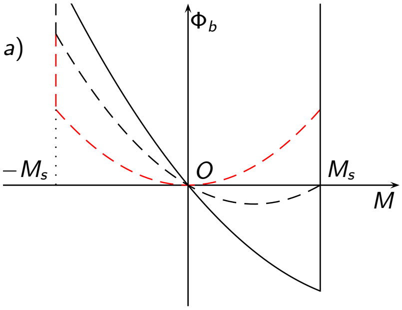

Figure: The graph of $\Phi_b(H, \cdot, \theta)$ and $\Phi_L(H, \cdot, \theta)$ at $\theta > \theta_c$ when $H = 2H^*$ (solid), $H = H^*/2$ (dashed), $H = 0$ (red dashed).

Non-convex potentials Φ: $\theta < \theta_c$, $\boxed{\tilde{H} > 0}$

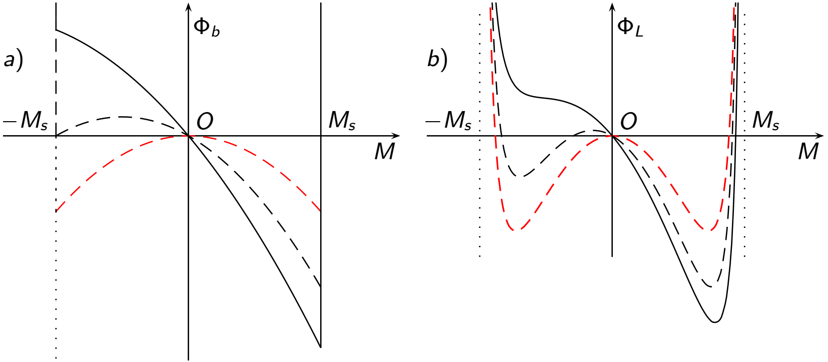

Figure: The graph of $\Phi_b(H,\cdot,\theta)$ and $\Phi_L(H,\cdot,\theta)$ at $\theta < \theta_c$ when $H = 2H^*$ (solid), $H = H^*/2$ (dashed), $H = 0$ (red dashed).

Non-convex potentials:

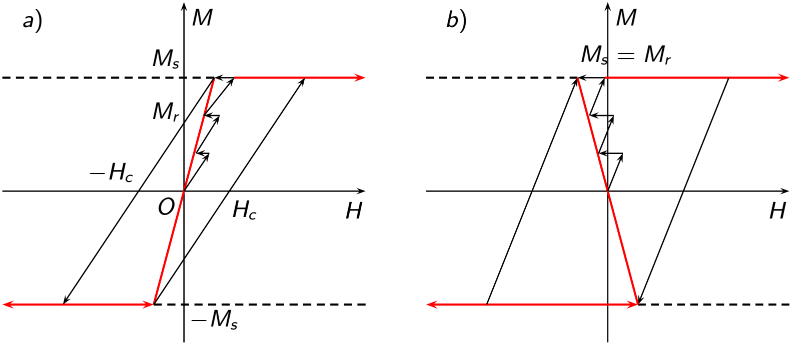

Figure: Minimum work expended: a) $\theta > \theta_c$ (convex) and b) $\theta < \theta_c$ (non-convex) . The skeleton curves in red.